Available online at www.sciencedirect.com

SciVerse ScienceDirect

Ceramics International 38 (2012) 4075–4079

CERAMICS INTERNATIONAL

www.elsevier.com/locate/ceramint

Template-free synthesis of neodymium hydroxide nanorods by microwave-assisted hydrothermal process, and of neodymium oxide nanorods by thermal decomposition

Anukorn Phuruangrat [a,*], Somchai Thongtem [b], Titipun Thongtem [c,**]

[a] Department of Materials Science and Technology, Faculty of Science, Prince of Songkla University, Hat Yai, Songkhla 90112, Thailand
[b] Department of Physics and Materials Science, Faculty of Science, Chiang Mai University, Chiang Mai 50200, Thailand
[c] Department of Chemistry, Faculty of Science, Chiang Mai University, Chiang Mai 50200, Thailand

Received 8 May 2011; received in revised form 21 January 2012; accepted 24 January 2012
Available online 1 February 2012

Abstract

Based on the 150 °C and 1 h microwave-assisted hydrothermal reaction of $Nd(NO_3)_3$ dissolved in deionized water with pH 10 adjusted by concentrated NH_4OH solution, the phase and morphology of the product, characterized by XRD, SEM and TEM analyses, were specified as hexagonal $Nd(OH)_3$ nanorods 50 nm in diameter and 700 nm long, growing along the [0 0 1] direction. TGA analysis showed the evaporation of adsorbed water and dehydration of $Nd(OH)_3$ to synthesize the final pure Nd_2O_3 product. With 500 °C and 2 h calcination of the $Nd(OH)_3$ self-template precursor, Nd_2O_3 nanorods were synthesized, retaining both the morphology and growth direction of the precursor.

Keywords: A. Microwave processing; A. Calcination; B. Electron microscopy; B. X-ray methods; Nanorods

1. Introduction

Since the discovery of carbon nanotubes (CNTs), a new structured carbon, in 1991 [1], one-dimensional (1D) nanostructures such as nanorods, nanowires, nanobelts and nanotubes have been promising materials for various electronic, optoelectronic, magnetic and photonic devices due to their unique physical and chemical properties – quite different from those of the corresponding bulk materials [2–4]. Rare earth oxides have been used in a number of scientific areas, such as ceramic industries, and as catalysts for dehydrogenation, hydrogenation and esterification reactions, arising from their 4f electrons [2,5–9]. Among these, neodymium oxide (Nd_2O_3) has been widely used in luminescent materials for photonic applications, as a catalyst for the synthesis of ammonia and the oxidative coupling of methane, and as a protective coating [7,10]. Therefore, the preparation and characterization of Nd_2O_3 nanorods have attracted much interest in recent years. There are many reports on the synthesis of rare earth oxides with different morphologies, i.e. the synthesis of: uniform nanorods, nanowires and nanoplates of rare earth oxides (M_2O_3, M = Pr, Nd, Sm, Eu, Gd, Tb and Dy) by microwave irradiation [5]; Nd_2O_3 nanowires through a sol–gel process assisted by a porous anodic aluminum oxide (AAO) template [6]; rare earth oxide nanoparticles of Sm and Nd by hydrogen plasma-metal reaction [7]; $Ln(OH)_3$ (Ln = La, Pr, Nd, Sm, Eu and Gd) by a simple wet chemical method [8]; Nd_2O_3 nanopowders by sol–gel auto-combustion [9]; Nd_2O_3 nanoparticles by a tartrate route [10]; and Nd_2O_3 nanoparticles [11] and rod-like Eu:Gd_2O_3 phosphor [12] via a hydrothermal route.

In the present research, we report the template-free synthesis of $Nd(OH)_3$ nanorods by the 150 °C and 1 h microwave-assisted hydrothermal (MH) reaction of $Nd(NO_3)_3$ solution with pH 10 adjusted by concentrated NH_4OH solution – a novel, facile, fast and environmentally benign low-temperature process. Subsequently, the $Nd(OH)_3$ nanorod self-template precursor was further calcined at 450 and 500 °C for 2 h to form Nd_2O_3 nanorods. This success may lead to large-scale synthesis applicable for a number of industries.

* Corresponding author. Tel.: +66 (0)74 288 374; fax: +66 (0)74 288 395.
** Corresponding author. Tel.: +66 (0)53 943 344; fax: +66 (0)53 892 277.
E-mail addresses: phuruangrat@hotmail.com (A. Phuruangrat), ttpthongtem@yahoo.com (T. Thongtem).

0272-8842/$36.00
doi:10.1016/j.ceramint.2012.01.065

2. Experimental procedure

Neodymium (III) nitrate ($Nd(NO_3)_3$) and ammonium hydroxide (NH_4OH) were purchased from Sigma–Aldrich Co., and used without further purification. In a typical synthesis, 50 ml of aqueous 0.01 M $Nd(NO_3)_3$ was adjusted the pH to 10 by concentrated NH_4OH solution. It was transferred into a 100 ml Teflon-lined stainless-steel autoclave, which was filled with deionized water up to 80% total capacity. The system was heated by 0–100% 300 W microwave from room temperature to 150 °C for 20 min, held at this temperature for 1 h, and left cool down to room temperature. The resulting product was filtered, washed with distilled water and absolute ethanol, and dried at 80 °C for 12 h. Then the filtered product, the self-template precursor, was further calcined at the rate of 5 °C min^{-1} to 450, 500 and 550 °C and held at each of these temperatures for 2 h in ambient atmosphere to synthesize the final powders.

The weight loss (less), purified phase, structure and morphology of the as-synthesized products were characterized by a Shimadzu Scientific Instruments TGA-50 Thermogravimetric (TGA) analyzer under a stream of nitrogen at a heating rate of 10 °C min^{-1}, a Bruker AXS D8 Advance Powder X-ray diffractometer (XRD) with K_α line from a copper target, a JEOL JSM-6335F field emission scanning electron microscope (FE-SEM) operating at 15 kV accelerating voltage with Au sputtering on the samples, and a JEOL JEM-2100F transmission electron microscope (TEM) and high resolution transmission electron microscope (HRTEM) including selective area electron diffractometer (SAED) operating at the accelerating voltage of 200 kV.

3. Results and discussion

Fig. 1 shows the thermogravimetric analysis (TGA) curve of the $Nd(OH)_3$ precursor. It shows continuous weight loss over a range of 50–650 °C, with a total weight loss of 15.44%. Theoretically, $Nd(OH)_3$ decomposes to form Nd_2O_3 and H_2O:

$$2Nd(OH)_3 \rightarrow Nd_2O_3 + 3H_2O \quad (1)$$

Under the molar conservation of the (1) reaction, the calculated weight loss is 13.84%, lower than that from TGA analysis. The precursor might absorb some moisture (water vapor) from the ambient atmosphere, which would evaporate during TGA analysis. The weight loss of the $Nd(OH)_3$ precursor was classified into three steps. First, weight loss in the temperature range of 50–270 °C was specified as the decomposition of adsorbed residual water on the surface of $Nd(OH)_3$. Second, weight loss at the temperature range 270–430 °C was due to the dehydration of $Nd(OH)_3$ to form NdOOH. Third, weight loss at 430–650 °C corresponded to the well-defined NdOOH dehydration into a hexagonal Nd_2O_3 structure [12–14]. In the present research, the TGA weight loss (Table 1) was very close to the theoretical value calculated from the molar conservation of products and reactants of the (2) and (3) chemical reactions [12]. The dehydration of $Nd(OH)_3$ to form Nd_2O_3 can be written as follows:

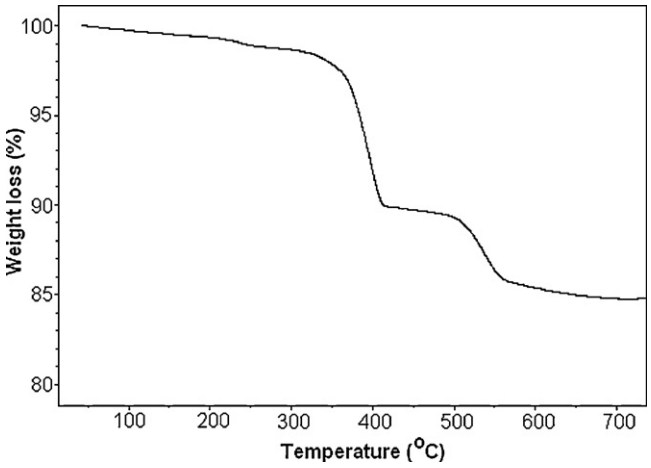

Fig. 1. TGA curve of $Nd(OH)_3$ precursor synthesized by the 150 °C and 1 h MH process.

$$2Nd(OH)_3 \rightarrow 2NdOOH + 2H_2O \quad \text{at} 270-430\,^\circ C \quad (2)$$

$$2NdOOH \rightarrow Nd_2O_3 + H_2O \quad \text{at} 430-650\,^\circ C \quad (3)$$

The different phases of the products were analyzed by X-ray diffraction, as shown in Fig. 2. All diffraction peaks of the as-synthesized precursor were indexed as pure phase of hexagonal $Nd(OH)_3$, JCPDS No. 70-0214 [14]. Its diffraction peaks were at 2θ of 16.06, 27.90, 28.94, 32.34, 37.13, 40.59, 48.65, 49.26, 50.01, 57.11, 65.55, 71.73 and 79.42°, which were assigned as the (1 0 0), (1 1 0), (1 0 1), (2 0 0), (1 1 1), (2 0 1), (0 0 2), (3 0 0), (2 1 1), (1 1 2), (1 3 1), (3 0 2) and (2 3 1) planes, respectively. Upon calcination at 450, 500 and 550 °C for 2 h, the peaks were at 2θ of 26.88, 29.82, 30.80, 40.52, 47.44, 53.54, 57.00, 57.67, 61.89, 64.14, 68.76, 74.29 and 77.83°, specified as the (1 0 0), (0 0 2), (0 1 1), (0 1 2), (1 1 0), (1 0 3), (1 1 2), (2 0 1), (0 0 4), (2 0 2), (0 1 4), (0 2 3) and (1 2 1) planes of pure hexagonal Nd_2O_3 phase, in accordance with JCPDS No. 75-2255 [14]. Atomic diffusion became more violent with an increase in calcination temperature.

In microwave-assisted hydrothermal (MH) synthesis, the final morphology of the product was controlled by surface chemistry, resulting in either oriented or random attachment of particles. During the MH process, Nd^{3+} ions reacted with

Table 1
Weight loss of $Nd(OH)_3$ precursor characterized by TGA at 50–650 °C.

Temperature range (°C)	Reaction	TGA weight loss (%)	Theoretical weight loss (%)
50–270	Dehydration of water on $Nd(OH)_3$ surface	1.23	–
270–430	$2Nd(OH)_3 \rightarrow 2NdOOH + 2H_2O$	8.91	9.23
430–650	$2NdOOH \rightarrow Nd_2O_3 + H_2O$	5.30	4.61

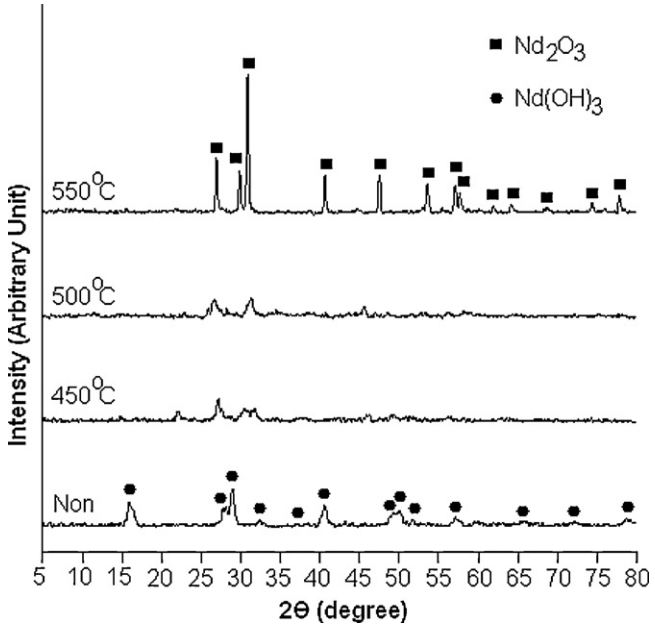

Fig. 2. XRD patterns of $Nd(OH)_3$ precursor, and Nd_2O_3 synthesized by the 450, 500 and 550 °C calcination of its precursor for 2 h.

hydroxyl ions of NH_4OH to form $Nd(OH)_3$ nanorods:

$$Nd^{3+} + 3OH^- \rightarrow Nd(OH)_3 \quad (4)$$

In general, the morphology of the product was determined by the rates of nucleation and crystal growth, which were controlled by the inherent crystal structure and chemical potential of the precursor solution [15,16]. When the rate of nucleation was greater than that of crystal growth, the crystal size as well as its aspect ratio would be small. In contrast, fast crystal growth would lead to a large crystal with a high aspect ratio along the preferential direction [15]. At a high concentration of hydroxyl ions, the reaction of Nd^{3+} and OH^- to form $Nd(OH)_3$ was very fast, and the aggregation of particles led to the formation of nanorods. The concentrations of Nd^{3+} and OH^- were high enough to form $Nd(OH)_3$ in the shape of nanorods. Further calcination of $Nd(OH)_3$ nanorods in a furnace at 450–550 °C led to the dehydration process, with the formation of Nd_2O_3 by the following reaction:

$$2Nd(OH)_3 \rightarrow Nd_2O_3 + 3H_2O \quad (5)$$

Under the optimum conversion condition (500 °C and 2 h), the final geometry of Nd_2O_3 nanorods was predetermined by the shape and size of the $Nd(OH)_3$ nanorods, functioning as self-template precursors.

Morphologies of the products were characterized by SEM, as shown in Fig. 3. Fig. 3a shows $Nd(OH)_3$ nanorods 700 nm long and 50 nm in diameter. The growth of $Nd(OH)_3$ nanorods was reliable in the reaction system without any catalyst, template or surfactant. The anisotropic growth of $Nd(OH)_3$ was mainly controlled by the inherent crystal structure and chemical potential of the solution [16]. For the crystal structure of $Nd(OH)_3$, all of the positive Nd^{3+} cations reside on the (0 0 1) face, with most of their dangling bonds coordinated with OH^- anions, alternately stacking along the [0 0 1] direction. Compared with the (1 1 0) and (1 0 0) planes, they have fewer ions with weaker polarity than the (0 0 1) plane. This characteristic structure promotes the highest density of Nd^{3+} and OH^- ions along the [0 0 1] direction,

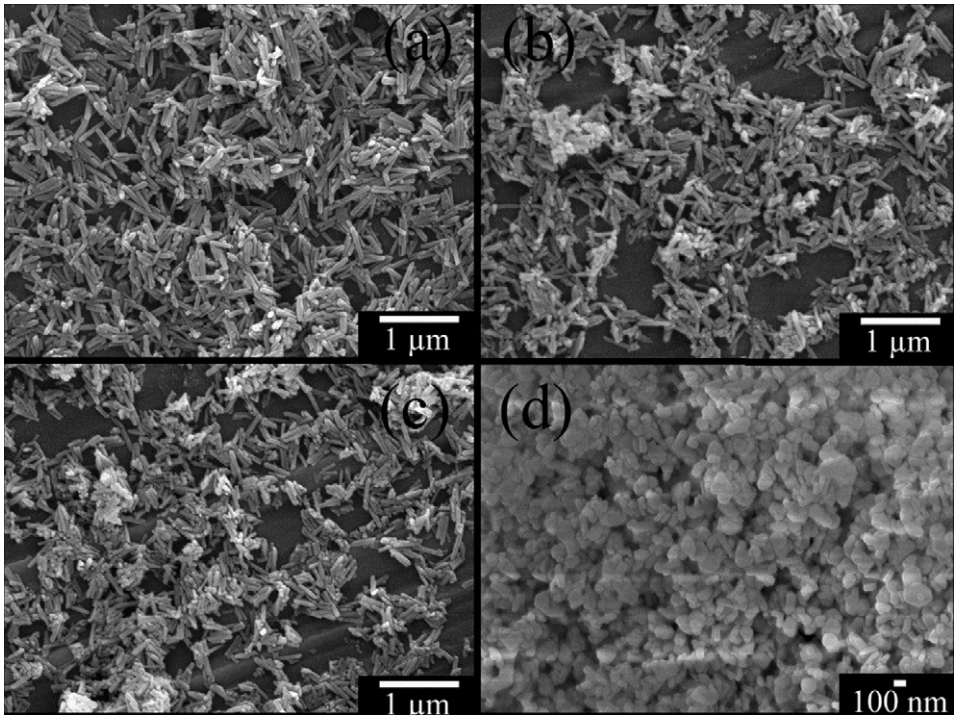

Fig. 3. SEM images of (a) $Nd(OH)_3$ nanorods synthesized by the 150 °C and 1 h MH process and (b–d) Nd_2O_3 synthesized by the 450, 500 and 550 °C calcination of $Nd(OH)_3$ precursor for 2 h, respectively.

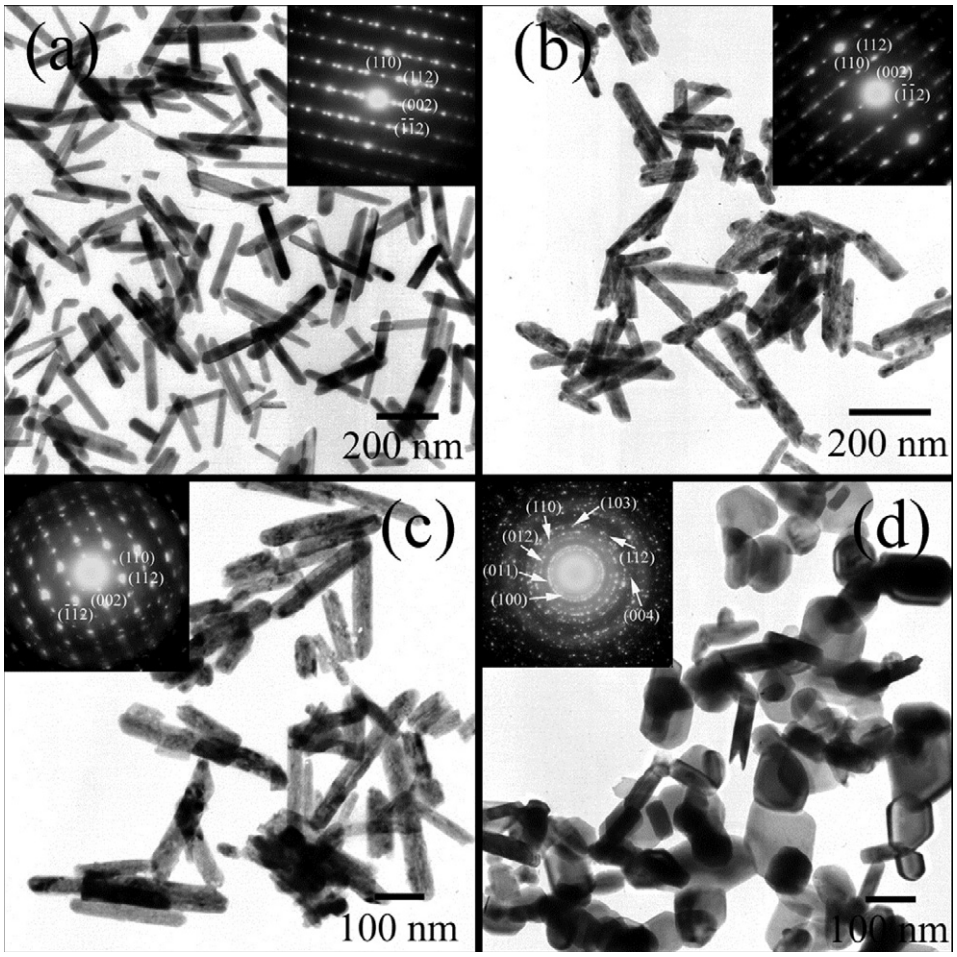

Fig. 4. TEM images and SAED patterns of (a) $Nd(OH)_3$ nanorods synthesized by the 150 °C and 1 h MH process and (b–d) Nd_2O_3 synthesized by the 450, 500 and 550 °C calcination of $Nd(OH)_3$ precursor for 2 h, respectively.

which leads the (0 0 1) face to have the highest chemical potential and the most activity in relation to the surrounding growth conditions. Thus, the final crystal morphology is cooperative with the internal crystal structure and external reaction conditions [8]. It should be noted that calcination temperature was an important factor in determining the average particle size of the product. The particle size of Nd_2O_3 was increased with increasing calcination temperature. The degree of crystallinity was also increased. SEM analysis shows nanorod shapes with an estimated size of ∼70 nm in diameter and ∼500 nm in length from calcination at 450 and 500 °C for 2 h. Upon increasing the calcination temperature to 550 °C, but keeping the length of time at 2 h, they changed to nanoparticles with their sizes range of 80–200 nm.

TEM images of $Nd(OH)_3$ and Nd_2O_3 are shown in Fig. 4. The $Nd(OH)_3$ crystallites, synthesized by the microwave-assisted hydrothermal process, displayed uniform nanorods 20–40 nm in diameter and 200–400 nm in length (Fig. 4a). The morphology was almost the same when the $Nd(OH)_3$ precursor was calcined at either 450 °C or 500 °C for 2 h. But for 550 °C and 2 h calcination, the product became nanoparticles with an average size of 100 nm. At these stages, water evaporated and atomic diffusion proceeded. Selected area electron diffraction (SAED) patterns (insets of Fig. 4a–c) of the individual products corresponded to the (1 1 0), (1 1 2), (0 0 2) and (−1 −1 2) planes with [2 –2 0] as the zone axis, and were specified as $Nd(OH)_3$ and Nd_2O_3 single crystals [14] in accordance with the above XRD analysis. It should be noted that the planes of $Nd(OH)_3$ and Nd_2O_3 single crystals were the same, but their 2θ Bragg's angles were different. At 550 °C for 2 h, the SAED pattern (inset of Fig. 4d) was composed of concentric rings of bright spots, characterized as polycrystal. The interpreted pattern corresponded to the (1 0 0), (0 1 1), (0 1 2), (1 1 0), (1 0 3), (1 1 2) and (0 0 4) planes of Nd_2O_3 [14]. Fig. 5 shows typical HRTEM images of $Nd(OH)_3$ and Nd_2O_3 nanorods. Clearly, Fig. 5a reveals only d-spacing of the (1 1 0) and (2 0 0) planes, with a lattice spacing of about 0.321 and 0.278 nm for an individual $Nd(OH)_3$ nanorod. The HRTEM result suggested that the $Nd(OH)_3$ nanorod grew along the [0 0 1] direction, making angles of about 60° and 0° with the (1 1 0) and (2 0 0) lattice planes, respectively. Fig. 5b shows the 0.332 nm interplanar space, corresponding to d-spacing of the (1 0 0) plane of an individual Nd_2O_3 nanorod, parallel with its [0 0 1] growth direction.

4. Conclusions

Uniform Nd_2O_3 nanorods were successfully synthesized by the 500 °C and 2 h calcination of a $Nd(OH)_3$ nanorod precursor,

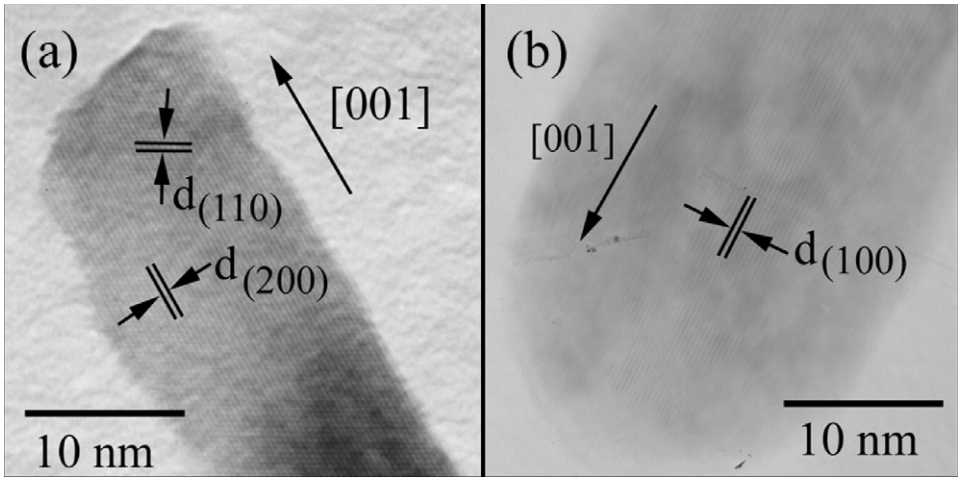

Fig. 5. HRTEM images of (a) $Nd(OH)_3$ nanorod synthesized by the 150 °C and 1 h MH process and (b) Nd_2O_3 nanorod synthesized by the 500 °C and 2 h calcination of $Nd(OH)_3$ nanorod precursor.

which was synthesized by a one-step MH method at 150 °C for 1 h. Based on the experimental results, the final morphology of the one-dimensional (1D) Nd_2O_3 nanostructure was controlled by the morphology of the $Nd(OH)_3$ self-template nanorod and the calcination temperature. A possible growth mechanism of $Nd(OH)_3$ 1D nanorods was proposed, in which the growth was promoted by the highest number of Nd^{3+} and OH^- ions along the [0 0 1] direction.

Acknowledgments

We wish to thank the National Nanotechnology Center (NANOTEC), National Science and Technology Development Agency, for providing financial support through the project P-10-11345, the Thailand's Office of the Higher Education Commission through the National Research University (NRU) Project, and the Thailand Research Fund through the TRF Research Grant.

References

[1] S. Iijima, Helical microtubules of graphitic carbon, Nature 354 (1991) 56–58.
[2] N. Zhang, R. Yi, L. Zhou, G. Gao, R. Shi, G. Qiu, X. Liu, Lanthanide hydroxide nanorods and their thermal decomposition to lanthanide oxide nanorods, Mater. Chem. Phys. 114 (2009) 160–167.
[3] X. Wang, Y. Li, Solution-based synthetic strategies for 1D nanostructures, Inorg. Chem. 45 (2006) 7522–7534.
[4] H. Guan, Y. Zhang, Hydrothermal synthesis and characterization of hexagonal and monoclinic neodymium orthophosphate single-crystal nanowires, J. Solid State Chem. 177 (2004) 781–785.
[5] A.B. Panda, G. Glaspell, M.S. El-Shall, Microwave synthesis and optical properties of uniform nanorods and nanoplates of rare earth oxides, J. Phys. Chem. C 111 (2007) 1861–1864.
[6] X. Qu, J. Dai, J. Tian, X. Huang, Z. Liu, Z. Shen, P. Wang, Syntheses of Nd_2O_3 nanowires through sol–gel process assisted with porous anodic aluminum oxide (AAO) template, J. Alloys Compd. 469 (2009) 332–335.
[7] T. Liu, Y. Zhang, H. Shao, X. Li, Synthesis and characteristics of Sm_2O_3 and Nd_2O_3 nanoparticles, Langmuir 19 (2003) 7569–7572.
[8] L. Qian, Y. Gui, S. Guo, Q. Gong, X. Qian, Controlled synthesis of light rare-earth hydroxide nanorods via a simple solution route, J. Phys. Chem. Solids 70 (2009) 688–693.
[9] W. Yang, Y. Qi, Y. Ma, X. Li, X. Guo, J. Gao, M. Chen, Synthesis of Nd_2O_3 nanopowders by sol–gel auto-combustion and their catalytic esterification activity, Mater. Chem. Phys. 84 (2004) 52–57.
[10] B. Zhaorigetu, G. Ridi, L. Min, Preparation of Nd_2O_3 nanoparticles by tartrate route, J. Alloys Compd. 427 (2007) 235–237.
[11] L. Kępiński, M. Zawadzki, W. Mišta, Hydrothermal synthesis of precursors of neodymium oxide nanoparticles, Solid State Sci. 6 (2004) 1327–1336.
[12] C. Chang, F. Kimura, T. Kimura, H. Wada, Preparation and characterization of rod-like Eu:Gd_2O_3 phosphor through a hydrothermal routine, Mater. Lett. 59 (2005) 1037–1041.
[13] T. Thongtem, A. Phuruangrat, D.J. Ham, J.S. Lee, S. Thongtem, Controlled Gd_2O_3 nanorods and nanotubes by the annealing of $Gd(OH)_3$ nanorod and nanotube precursors and self-templates produced by a microwave-assisted hydrothermal process, CrystEngComm 12 (2010) 2962–2966.
[14] Powder Diffract. File, JCPDS-ICDD, 12 Campus Boulevard, Newtown Square, PA 19073-3273, U.S.A., 2001.
[15] W.B. Hu, D.T. Tian, Y.Z. Mi, G.H. Nie, Y.M. Zhao, Z.L. Liu, K.L. Yao, Synthesis and characterization of In_2O_3 nanocube via a solvothermal-calcination route, Mater. Chem. Phys. 118 (2009) 277–280.
[16] X. Wang, Y. Li, Synthesis and characterization of lanthanide hydroxide single-crystal nanowires, Angew. Chem. Int. Ed. 41 (2002) 4790–4793.